Individual Brain Charting dataset extension, fourth release of high-resolution fMRI data for cognitive mapping

Juan Jesus Torre, Ana Luísa Pinho, Swetha Shankar, Alexis Amadon, Mani Saignavongs, Marcela Perrone-Bertolotti, Thomas Bazeille, Elvis Dohmatob, Isabelle Denghien, Chantal Ginisty, et al.

Individual Brain Charting dataset extension, fourth release of high-resolution fMRI data for cognitive mapping

Juan Jesús Torre[1*], Ana Luísa Pinho[1], Swetha Shankar[1], Alexis Amadon[2], Mani Saignavongs[3,4], Marcela Perrone-Bertolotti[3,5], Thomas Bazeille[1], Elvis Dohmatob[1,16], Isabelle Denghien[6], Chantal Ginisty[7], Séverine Becuwe-Desmidt[7], Séverine Roger[7], Yann Lecomte[7], Valérie Berland[7], Laurence Laurier[7], Véronique Joly-Testault[7], Gaëlle Médiouni-Cloarec[7], Christine Doublé[7], Bernadette Martins[7], Jean-Philippe Lachaux[5], Patrick G. Bissett[8], Ayse Zeynep Enkavi[9], Ian Eisenberg[8], Russell Poldrack[8], Roberta Santoro[10,11,12], Elia Formisano[10,11,13], Gaël Varoquaux[1], Stanislas Dehaene[6,14], Lucie Hertz-Pannier[7,15], and Bertrand Thirion[1*]

[1]**Université Paris-Saclay, Inria, CEA, Palaiseau, 91120, France**
[2]**Université Paris-Saclay, CEA, CNRS, BAOBAB, NeuroSpin, 91191, Gif-sur-Yvette, France**
[3]**Lyon Neuroscience Research Center, INSERM U1028 / CNRS UMR 5292, Lyon, France**
[4]**Epilepsy Institute IDEE, Lyon, France**
[5]**University Claude Bernard, F-69000 Lyon, France**
[6]**Cognitive Neuroimaging Unit, INSERM, CEA, Université Paris-Saclay, NeuroSpin center, 91191 Gif/Yvette, France**
[7]**Université Paris-Saclay, CEA, UNIACT, NeuroSpin, 91191, Gif-sur-Yvette, France**
[8]**Department of Psychology, Stanford University, CA 94305, United States**
[9]**Division of Humanities and Social Sciences, Caltech, CA 91125, United States**
[10]**Department of Cognitive Neuroscience, Faculty of Psychology and Neuroscience, Maastricht University, 6200 MD Maastricht, The Netherlands**
[11]**Maastricht Brain Imaging Center, 6200 MD Maastricht, The Netherlands**
[12]**Brain and Language Laboratory, Department of Clinical Neuroscience, University Medical School, University of Geneva, CH-1211 Geneva, Switzerland**
[13]**Maastricht Centre for Systems Biology, Maastricht University, 6200 MD Maastricht, The Netherlands**
[14]**Collège de France, Université Paris-Sciences-Lettres, Paris, France**
[15]**UMR 1141, NeuroDiderot, Université de Paris, France**
[16]**Criteo AI Lab, France**
[*]**Corresponding authors: juan-jesus.torre-tresols@inria.fr, bertrand.thirion@inria.fr**

Abstract

Functional Magnetic Resonance Imaging (fMRI) constitutes the primary imaging technique that allows us to investigate brain-functional organization at the millimeter scale. We thus present herein another extension of the *Individual Brain Charting* (IBC) dataset – a long-running project dedicated to map cognition in twelve individuals brains. In this release, we provide more multi-task fMRI data at high-spatial resolution –i.e. 1.5mm– from the same individuals. Concretely, the data refer to the performance of eighteen distinct tasks across seven fMRI sessions, comprising a wide range of cognitive processes. The data release pertains to both raw data and derived statistical maps that can be found in *OpenNeuro* plus *EBRAINS* and *NeuroVault*, respectively. In addition to fMRI, we provide paradigm descriptors of the tasks' designs compliant with the Brain Imaging data Structure (BIDS) conventions, as well as code to reproduce the tasks.

Keywords

Brain mapping, fMRI, Neuroimaging

Introduction

Imaging-based brain mapping is a central tool to understand the principles that govern brain function, as it allows the delineation of functional regions and their underlying network structure.

From the wide range of imaging techniques available, *functional Magnetic Resonance Imaging* (fMRI) stands out for this endeavor; the combination of its mm-scale spatial resolution and non-invasiveness make it the standard for brain mapping. Although extensive literature has been published on the functional mapping of specific brain areas, the number of studies aiming at understanding the brain as a whole is much more scarce. Some efforts towards this later objective are meta- and mega- analyses, commonly used in many other scientific fields [14]. They allow the study of accumulated data, by pooling together results from different studies, which in turn facilitates the investigation of brain systems linked to cognitive processes. Several studies have outlined both the pros and cons of meta-analyses [47, 5]. Potential benefits include the reduction of possible false positives and false negatives that can be found in individual studies. Others have pointed to the lack of general guidelines for these types of analyses in neuroimaging, and made an effort to propose such principles, [22] proposes ten guidelines for neuroimaging meta-analyses in particular, from being specific with the research question to controlling for multiple contrasts and reporting how the data was gathered and organized. Besides, large-scale neuroimaging-data studies have been used to address "brain signatures" of processes such as pain [46], as well as to create brain atlases of cognition [40, 39, 44].

Still, certain features of these types of analyses, such as the underlying inter-subject and inter-site variability, limit the generalization of such findings. Besides the variability introduced by different cohorts, equipment plus experimental procedures across studies as well as the lack of standardized data-processing pipelines constitute further barriers for these methods to be used for brain atlasing. Recently, many efforts have been put forward with respect to overcoming the aforementioned limitations, such as the development of large-scale brain-imaging datasets. As not all the brain mapping limitations can be overcome simultaneously, each project has its own scope. For instance, the *CONNECT/Archi* [29, 28] and *Human Connectome Project* (HCP)[3, 11] and datasets focus on sample size and different imaging modalities, being ideal for population analysis. However, the number of total task-fMRI conditions in these datasets is scarce for functional atlasing (28 and 24, respectively). Another example is the *studyforrest* dataset [17, 18, 16, 41], which focuses on naturalistic stimuli and includes a rich variety of task data on complex auditory and visual information. Functional mapping of individual brains over different psychological domains is necessary achieve a wide brain coverage at a fine scale while maximizing the number of cognitive features included. Within this context, the *Individual Brain Charting* (IBC) project intends to develop a 1.5mm-resolution, task-fMRI dataset acquired in a fixed environment, on a permanent cohort of twelve participants. Collecting data from a broad range of tasks allows for a sharp characterization of the neurocognitive components common to the different tasks.

The present extension of the dataset corresponds to the fourth release of the IBC dataset, aiming to expand the functional coverage of previous releases [30]. The first release included modules ranging from all levels of cognition, including retinotopy, tonotopy, somatotopy, calculation, language and social reasoning [29, 3, 19]. The second one focused on higher-level cognition, like mental-time travel, reward, theory-of-mind, self-reference effect and speech recognition. Still, some tasks dedicated to lower-level processes, including pain, attention control and numerosity, are included. The third release contains data on retinotopy and naturalistic stimuli, namely movie-watching protocols and visualization of real-life video clips. This new release features two experimental batteries: one of them centered on self-control and the other one included a wide range of cognitive processes, including elementary motor functions, object salience, verbal and spatial working memory, and mapping of visual categories, among others. There is also an auditory task aimed at mapping different kinds of naturalistic auditory stimuli, with categories like animals, human voice, tools and nature sounds.

In total, data from all releases are organized in 46 tasks – most of them reproduced from previous studies– amounting for 216 contrasts described on the basis of 137 cognitive atoms, extracted from the *Cognitive Atlas* [35].

As we keep up our efforts to increase the functional coverage of the IBC dataset, more data releases are expected in the upcoming years. In the long term, we aim at building a deep-phenotype data resource that will enable a complete characterization of behavior and corresponding cognitive mechanisms in terms of brain function. Such facility can be instrumental on the development of future human-brain-atlasing frameworks as means to further the investigation and our understanding on the principles governing functional organization in the human brain. Also, we believe that openly sharing data and code resources is key to advance together as a scientific community; we therefore focus our efforts in making these resources available and well-documented for anyone who might want to use them.

Materials and Methods

Participants

The present release of the IBC dataset consists of brain fMRI data from eleven individuals (one female) with mean age equal to 34 (SD=5). One of the eleven (participant 1) is missing the data from the Stanford battery and Realistic sounds task. Data from the remaining participant are currently missing and they will be acquired in the future and included in one of the upcoming releases.

Table 1. List of the conditions for each task in the Lyon battery. The whole battery was acquired in two accquisition sessions, with four tasks per session. Each task was acquired twice to account for phase-encoding direction distortions.

Task	Contrast	Description
MOTO	hand_left	Left hand movement
	hand_right	Right hand movement
	finger_left	Left finger movement
	finger_right	Right finger movement
	saccade_left	Eye movement to the left
	saccade_right	Eye movement to the right
	foot_left	Left feet movement
	foot_right	Right feet movement
	tongue_left	Tongue movement to the left
	tongue_right	Tongue movement to the right
MCSE	hi_salience_left	High salience, target on the left
	hi_salience_right	High salience, target on the right
	low_salience_left	Low salience, target on the left
	low_salience_right	Low salience, target on the right
MVIS	2_dots	2 positions to remember
	4_dots	4 positions to remember
	6_dots	6 positions to remember
	X_dots_control	1 position to remember
MVEB	2_letters	2 different characters
	4_letters	4 different characters
	6_letters	6 different characters
	X_letters_same	1 character repeated X times
AUDI	speech	Speech in French
	reverse	French speech in reverse
	suomi	Speech in Suomi
	music	Real-life music sounds
	yawn	Concatenated sounds of people yawning
	environment	Real-life environmental sounds
	silence	Silence, used as baseline
	tear	Concatenated sounds of people crying
	cough	Concatenated sounds of people coughing
	animal	Real-life animal sounds
	alphabet	French voice saying the alphabet
	human	Other human sounds
LEC1	words	A word is presented
	pseudowords	A pseudoword is presented
	strings	A random string is presented
LEC2	attend	Word that has to be attended
	ignore	Word that has to be ignored
VISU	character	String of random characters
	house	Pictures of houses from the outside
	animal	Animal pictures
	target_fruit	Images of fruits
	pseudoword	Strings of characters forming a pseudoword
	face	Images of faces
	scene	Images of natural landscapes
	scrabled	Noisy image without any objects in it
	tool	Pictures of tools

Table 2. List of conditions for each task of the Stanford battery and Realistic sounds task. The Stanford battery was acquired in three accquisition sessions, with three tasks per session. Each task was acquired twice to account for phase-encoding direction distortions. Regarding the Realistic sounds task, it was acquired in two acquistion sessions, with six runs of the task each. The six runs of each session were split in two phase-encoding directions to compensate for distorsions.

Task	Contrast	Description
Stop Signal	go	Response trials
	stop	Inhibition trials
Two-by-Two	task_stay_cue_stay	No switch in task or cue
	task_stay_cue_switch	Only cue switches
	task_switch_cue_switch	Both switch
Stroop	congruent	Both word and color are the same
	incongruent	Color and word are not the same
Motor Selective SS	go_critical	Response trials (critical side)
	go_noncritical	Response trials (non-critical side)
	stop	Inhibition trials
	ignore	Ignore stop signal
Attention	spatial_congruent	The stim is cued, and flankers are congruent with target
	spatial_incongruent	The stim is cued, and flankers are incongruent with target
	double_congruent	The stim is not cued, flankers are congruent with target
	double_incongruent	The stim is not cued, flankers are incongruent with target
Discount	delay	Amount of delay in days
	amount	Amount of money offered
Ward and Aliport	PA_with_intermediate	Partially ambiguous with intermediate step
	PA_without_intermediate	Partially ambiguous without intermediate step
	UA_with_intermediate	Unambiguous with intermediate step
	UA_without_intermediate	Unambiguous without intermediate step
Dot Patterns	correct_cue_correct_probe	Correct pair of cue and probe
	correct_cue_incorrect_probe	Target cue with random incorrect probe
	incorrect_cue_correct_probe	Random incorrect cue with target probe
	incorrect_cue_incorrect_probe	Random incorrect cue and probe
Realistic Sounds	Voice	Non-language human sounds
	Animal	Animal sounds
	Tools	Sounds of tool usage
	Nature	Nature sounds
	Music	Music samples
	Speech	Human language sounds
	Catch	Sounds repeated from previous trial
	Silence	No sound, used as baseline

The cohort is predominantly right-handed, measured with the *Edinburgh Handedness Inventory* [23]. For more complete information on this, as well as in age and sex of the cohort, consult [30].

Stimuli

One unique aspect of the IBC dataset pertains to its strong emphasis in the taskwise dimension, allowing for a comprehensive brain coverage of cognitive-related mechanisms. As such, data releases comprise several distinct tasks and, in the present one, we provide data acquired during the performance of eighteen tasks, covering a wide range of cognitive processes. To this end, data is typically collected from already existing protocols that have been validated in previous work.

In the next sections, we present a brief description of the tasks featuring this release.

Lyon tasks battery

This group of tasks were originally used in a series of experiments by the Labex Cortex from the University of Lyon, France (for more information, consult https://labex-cortex.universite-lyon.fr/labex-cortex/version-anglaise/). All of them were designed for experiments using other imaging modalities, namely intracranial electroencephalography (iEEG), regular EEG or magnetoencephalography (MEG).

AUDI task [27]. The audio protocol comprises several categories of sounds, that are presented to the participant in samples of 12s, with 12s of rest between presentations. The sound categories are alphabet, speech (in French), suomi, reverse speech, tear (sounds of people crying), yawn, environmental sounds, animal sounds, music, silence, cough, human (non-speech human sounds) and alphabet (female voice reciting the alphabet in French).

LEC1 task [36]. In this task, the participant is presented with a display of three possible rows where words appear alternately, as indicated by two columns of plus signs. At the beginning of each block, one of the three rows turns white to cue that words will appear there. The task is different depending on the rows. For the top row, the participant must answer (always using two buttons) whether the words corresponds to a living creature or not. For the middle row, several pseudowords are displayed, and the participant must answer whether they are composed of one or two syllables. Lastly, the bottom row displays random strings of letters, and the participant must determine whether they are presented in lowercase or uppercase.

LEC2 task [27]. For this protocol, the participant is presented with a series of words displayed on the screen one by one, which can be in one of two colors: black or white. The participants are instructed to attend only to a group of letters, and ignore the other. Both sets of words compose a complete story on their own. The interval between word presentations is jittered and centered around 700 ms.

MCSE task [24]. A task intended to assess visual search under both low and high salience conditions. The display is divided in four quadrants, where a group of "L" letters and a single "T" target letter are presented in various degrees of inclination. The target letter is always colored in light grey, whereas the rest of the letters can be colored in black (high salience condition) or light grey as well (low salience condition).

MOTO task. This is a simple motor task that maps motor responses from different body parts, alternating left and right sides. The participants are shown a display with 3 grey squares in a black background. When one of the lateral squares turns white, the participant must move the corresponding body part (hand, finger, eyes, feet or tongue) to the corresponding side (left or right).

MVEB (*Verbal Working Memory Task*) task [15]. For this protocol, participants are presented with a string of characters that can contain up to 6 distinct letters. After a brief pause, a single letter is presented, and the participant must answer whether it was part of the aforementioned string or not. The string can be comprised of one (control), two, four or six different characters.

MVIS (*Visual Working Memory Task*) task [15]. Similarly to the MVEB task, participants are presented a 4×4 grid where a certain number of points (two, four or six) appear. After a short amount of time, the dots are removed and a single dot is presented somewhere in the grid. The participant's task is then to answer if the presented dot is in the same spot as any of those presented before.

In the control condition, one of the dots is highlighted, meaning that it is the only position the participant has to retain in memory.

VISU task [45]. This task consists in a series of images presented to the participant during 200 ms each. The participant is instructed to press a button whenever they see a target category (fruit). The other categories are: characters, house, animal, pseudoword, face, scene, scrambled, tool.

Stanford Self Control tasks

This battery of tasks aims at assessing several processes related to self-control. As with the rest of the tasks, some adaptations were performed to ensure adaptability to our equipment and region (e.g., changed monetary amounts from dollars to euros). It was developed in Poldrack's lab from Stanford University (https://poldracklab.stanford.edu/). In this case, the tasks were specifically designed for fMRI experiments.

Attention Network task [9]. This protocol is a version of the classic *Flanker task* [8], where the participant has to judge the direction of a target arrow surrounded by four other flankers that can point in the same direction as the target (congruent) or not (incongruent). Additionally, two types of cues could precede the flanker stimuli: either one cue (called spatial cue) would indicate where the flanker was going to appear, or two cues would appear at the same time in the two possible locations (double cue).

Columbia Cards task [10]. Participants are presented with a set of cards face down. In each trial, a different number of cards appear and the participant is informed of the amount gained per gain card uncovered, the amount lost when uncovering the loss card, and the number of bad cards in the set. The participant can uncover as many cards as they want, before pressing the button that validates their decision and goes to the next trial. Uncovering a loss card automatically ends the trial. The task consists of 88 trials divided in 4 blocks of 22 trials each. The total number of cards plus the number of bad cards changes at every trial as well as the amount gained per card uncovered and the amount lost if a bad card was

uncovered. The order of the cards' presentation is predetermined for each trial, although the participant is not aware of it.

Discount task [21]. The participant is presented with a series of hypothetical monetary choices. They can either accept 20 euros in the moment or rather wait a certain amount of days in order to receive a bigger amount. Both the second amount and the number of days to wait are different for each trial.

Dot Patterns expectancy task [25]. This task presents a pair of stimuli separated by a fixation cross. The stimuli are shapes composed of small circles. The first one is the "cue", and the second one is the "probe", and is always grey. The participant has to press a button as fast as possible after the presentation of the probe, and only one specific combination of cue-probe refers to a differentiated response. This specific combination is the target pair, and it is randomly selected for each participant at the beginning of the experiment.

Stop Signal task [4]. The participant is trained to respond to each of four possible geometrical figures with their index or middle fingers (two figures for each finger). In some cases, a red star-shape (stop signal) appears after the presentation of the target, meaning that the motor response has to be withheld. The delay between the shape and the stop signal increases as participants successfully stop and decreases as participants fail to stop (i.e., respond on stop trials)

Motor Selective Stop Signal [2]. This task is mostly identical to the previously described Stop Signal task. The difference is that the participant is instructed to only stop if the stop signal occurs and they were going to make one of their two responses (critical response), but ignore the signal if they were going to make the other response (non-critical response).

STROOP [6]. In this task, the participant is presented one of the following words: "RED", "BLUE" or "GREEN", that can be colored in any of the three colors. The answer has to correspond to the written word, and not to the color it is presented in. The main difference with the classic STROOP task [43] is that its pace is not determined by the participant.

Two-by-Two task [38]. Task-switching paradigm using a 2 by 2 cue-task correspondence. The participant is presented with numbers from 1 to 9 (excluding the number 5), which can be either orange or blue. Briefly before presenting the stimulus, the type of task is revealed where the number will appear. The two possible tasks are "color" or "magnitude" (lower or higher than 5). The participants have one button assigned to one of the possible responses for each task. It is also important to note that each of the two tasks has two possible cues: the "color" task can be also be indicated by the cue "orange/blue", and the "magnitude" task can be indicated by the "high/low" cue, thus the 2 by 2 task-cue mapping.

Ward and Aliport task [20]. This is a digital version of the *WATT3 task* [48], which is a modified version of the classic *Tower of London task* [42], and its main purpose is to capture activation related to planning abilities. Therefore, the task uses a factorial manipulation of 2 task parameters: search depth and goal hierarchy. Search depth involves mentally constructing the steps necessary to reach the goal state, and the interdependency between steps in order to do so. This is expressed by the presence or absence of intermediate movements necessary for an optimal solution of each problem. Goal hierarchy refers to whether the order in which the three balls have to be put in their goal positions can be completely extracted from looking at the goal state or if it requires the participant to integrate information between goal and starting states (which result in unambiguous or partially ambiguous goal states, respectively) Detailed descriptions together with examples of each of the four categories can be found in [20].

Realistic Sounds task (Audio)

This task, developed and validated by Elia Formisano's lab (https://mbic-auditorylab.nl/) in [37], consists in the presentation of several categories of sounds. The sounds last two seconds each, and the interval between sounds can be either four or six seconds. The participant is instructed to press a button whenever they hear the same sound twice. The categories are: animal, tool, speech, voice, environment, music, silence and catch (repeated sound).

The task was acquired over 12 runs with 72 trials each, plus 5 silence trials and 5 catch trials, making a total of 82 trials per run.

Procedures and stimulation setup

The majority of the protocols used in the IBC project are adapted from their original studies in order to e.g. ensure compatibility with the acquisition setup of our fixed environment. Additionally, we provide a comprehensive documentation that aims to ease transparency and usage of both neuroimaging data and task protocols (consult https://project.inria.fr/IBC/data/). Depending on the task, they were either adapted from previously existing protocols or re-implemented from scratch.

The list of software tools used for the tasks comprising these data are:

1. Lyon tasks: Presentation (Version 20.1, Neurobehavioral Systems, Inc., Berkeley, CA, www.neurobs.com)
2. Stanford tasks: JavaScript, Python
3. Realistic sounds task: Python

Functional MRI data acquisition

FMRI data were acquired using an MRI scanner Siemens 3T Magnetom Prisma^{fit} together with a Siemens Head/Neck 64-channel coil. Behavioral responses were registered with two MR-compatible, optic-fiber response

devices that were used depending on the task employed: *(1)* a five-button ergonomic pad (Current Designs, Package 932 with Pyka HHSC-1x5-N4); and *(2)* a pair of in-house custom-made sticks featuring one-top button. MR-Confon package was used as audio system in the MRI environment.

All sessions were conducted at the NeuroSpin platform of the CEA Research Institute, Saclay, France.

Sequences used during the data acquisition include a Gradient-Echo (GE) pulse, whole-brain Multi-Band (MB) accelerated Echo-Planar Imaging (EPI) T2*-weighted sequence with Blood-Oxygenation-Level-Dependent (BOLD) contrasts. Consult Table 3 for a list of the different sequences employed in each acquisition session.

Two different runs for the same task were always performed using two opposite phase-encoding directions: one from Posterior to Anterior (PA) and the other from Anterior to Posterior (AP). The purpose was to guarantee within-subject replication of each task, while reducing limitations that may arise from the distortion-correction procedure. Spin-Echo (SE) EPI-2D image volumes were acquired in order to correct for spatial distortions. Like the GE-EPI sequences, two different acquisitions were also performed using PA and AP phase-encoding direction.

The parameters for all types of sequences employed are provided in [30] as well as in the documentation available on the IBC website: https://project.inria.fr/IBC/data/.

Dataset Content

The present release of the IBC dataset refer to source (raw) MRI data concerning the tasks described in this paper, meta-data (including events files), derived statistical maps and all the stimulation material used to acquire the data (total 333 GB).

The dataset is organized following BIDS Specification version 1.4.0 [12].

Paradigm descriptors

For each MRI session, the paradigm descriptors for GLM estimation were extracted from the log of the experiment. They were saved as event files, following BIDS Specification. Scripts to obtain these events files are provided together with the experimental protocols (see Section "Data and Software Availability: Software").

fMRI data

The acquired DICOM images were converted to NIfTI format using the `dcm2nii` tool, which can be found at https://www.nitrc.org/projects/dcm2nii. During conversion to NIfTI, all images were fully anonymized: pseudonyms were removed and images were defaced using the `mri_deface` command line, from the Freesurfer-6.0.0 library. Source data were preprocessed using *PyPreprocess* (https://github.com/neurospin/pypreprocess).

The fMRI images for each session are available as unpreprocessed data, as well as statistical parametric maps summarizing the main effects per subject, together with the event files corresponding to each run.

Source code

One of the key goals of the IBC project is to create open data and make experiments reproducible. For that reason, we prepare the source code used to acquire all the released data ready to be used (see "Section Data and Software Availability" for more information). The repository containing the source code is divided by tasks, and each one contains several elements:

1. protocol: Contains the scripts to run the experiment, as well as a README file explaining how to adapt and run the experiment
2. paradigm_descriptors: Here instructions are given to extract relevant information from the logfiles generated by the protocols, and to obtain BIDS-formated files like the ones we provide in the dataset
3. instructions: Files with instructions that were given to the participants before the experiment (in French)

Dataset Validation

Data quality

As part of the quality control of the dataset, we controlled the six rigid body motion estimates of the brain per scan. The interval ranges approximately within $[-1, 1]$mm/degree, and those beyond 1mm/degree motion are rare (see Figure 1 for details). No acquisition was discarded due to excessive motion (>2mm/degree).

Also, we computed the temporal SNR (tSNR), defined as the mean of each voxels' time course divided by their standard deviation, on normalized and unsmoothed data averaged across all acquisitions (Figure 1). Its values are between 35 and 70 in the cortex. Given the high resolution of the data (1.5mm isotropic), such values are indicative of a good image quality.

Data Reproducibility

In order to assess the data quality of the Lyon and Stanford batteries, we compared group-level results obtained with the IBC data from those obtained in the original studies. When a direct comparison with the results from the original studies was not possible, we used *NeuroQuery* –a meta-analytic tool that produces brain maps from text queries [7] (https://neuroquery.org/query?text=salience+network). Concretely, group-level IBC contrast maps refer to the conjunction of individual z-maps with an average threshold $> 25\%$ across subjects and corrected for multiple comparisons

Table 3. Overview of the MRI sessions for the fourth release according to the imaging sequences employed for data acquisition. A BOLD-fMRI run refers to the acquisition of fMRI data for one task. Two BOLD runs, concerned with the PA- and AP- phase-encoding directions, were acquired for every task during a session. Two pairs of 2D Spin-Echo maps (PA/AP) were always acquired before and after the BOLD-fMRI runs.

Session ID	Modality	Task	Duration of each run (min:sec)	Repetitions
Lyon 1	2D Spin-Echo	-	00:31	PA(×2) + AP(×2)
	BOLD fMRI	MOTO	11:57	PA + AP
	BOLD fMRI	MCSE	05:53	PA + AP
	BOLD fMRI	MVEB	06:45	PA + AP
	BOLD fMRI	MVIS	05:55	PA + AP
Lyon 2	2D Spin-Echo	-	00:31	PA(×2) + AP(×2)
	BOLD fMRI	LEC1	06:19	PA + AP
	BOLD fMRI	LEC2	04:45	PA + AP
	BOLD fMRI	AUDI	11:33	PA + AP
	BOLD fMRI	VISU	05:45	PA + AP
Stanford 1	2D Spin-Echo	-	05:30	PA(×2) + AP(×2)
	BOLD fMRI	Stop Signal	05:50	PA + AP
	BOLD fMRI	Attention	11:20	PA + AP
	BOLD fMRI	Two-by-Two	11:33	PA + AP
Stanford 2	2D Spin-Echo	-	00:31	PA(×2) + AP(×2)
	BOLD fMRI	Stroop	05:50	PA + AP
	BOLD fMRI	Discount	11:20	PA + AP
	BOLD fMRI	Motor Selective SS	11:33	PA + AP
Stanford 3	2D Spin-Echo	-	00:31	PA(×2) + AP(×2)
	BOLD fMRI	Columbia Cards	08:00	PA + AP
	BOLD fMRI	Dot Patterns	12:18	PA + AP
	BOLD fMRI	Ward and Aliport	08:00	PA + AP
Audio 1	2D Spin-Echo	-	00:31	PA(×2) + AP(×2)
	BOLD fMRI	Realistic Sounds	09:10	PA(×3) + AP(×3)
Audio 2	2D Spin-Echo	-	00:31	PA(×2) + AP(×2)
	BOLD fMRI	Realistic Sounds	09:10	PA(×3) + AP(×3)

with an FDR rate set at 5%. The data analysis was performed using the *NiLearn* software package [1].

For the Lyon battery, all tasks were originally acquired using intra-cranial EEG. However, robust activation can be observed in pertinent brain areas for all the tasks: the *MOTO*, *AUDI* and *VISU* tasks, being those which map the most basic functions, show consistent activation in the different parts of the motor cortex, primary auditory cortex and visual cortex, respectively.

For the language tasks, we can observe strong activations for *LEC1* in visual areas, as well as in areas of the language network, such as the left inferior frontal gyrus and basal temporal areas (i.e. Word Form Area). However, *LEC2* fails to capture significant activation on inhibitory processes related to the process of ignoring one of the stories, and it does not show robust activation on the 'voice-selective' areas reported in its original work [27]. It is important to note that the modulations in activity captured in the original study are probably not strong enough to be detected by a group study in a small sample (n=11), especially after whole-brain analysis.

In the case of the *MCSE* task, the activations shown by our results capture, albeit with weaker intensity, the effect on areas of the dorsal attention network reported in the original work [24]. These are the Inferior Parietal Cortex (IPS), Dorsolateral Prefrontal Cortex (DLPFC) and Medial Frontal Gyrus (MFG).

Lastly, we can also observe strong parietal activation in the working memory tasks. In the map for the *MVIS* task, one can observe prominent activations in visual areas, accounting for the spatial nature of the task; on the other hand, activations in both frontal cortices are depicted in the map referring to the *MVEB* task, which reflects its verbal components. The mentioned contrasts can be seen in

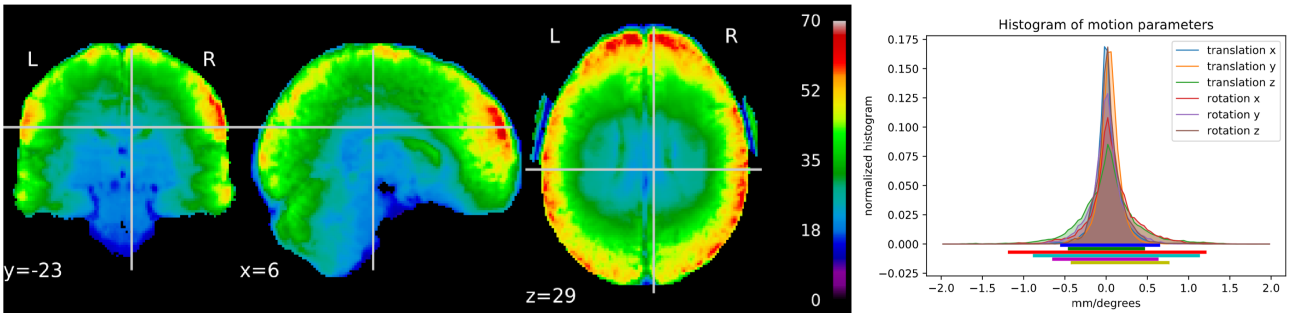

Figure 1. Data-quality assessment of the dataset. For all tasks and subjects, (left) tSNR varies between 35 and 70 in the cortex, with higher values registered in its upper layers, and (right) density of the six rigid-body parameters concerning head motion show that they remained confined to approximately 1.25mm/1degree across 99% of the images collected.

Figure 2.

Regarding the Stanford battery, only the original works for Motor Selective Stop Signal [2] and the Ward and Aliport [20] tasks included neuroimaging analysis. A selection of contrasts for this battery can be found in 3.

Starting with the aforementioned *Motor Selective Stop Signal*, we find clear activation for the stop-ignore condition in the right supplementary motor area, argued to process conflict resolution in the original study [2]. Weak activations are also found in some of the putative regions for the stop condition (primary sensory cortex, right inferior frontal cortex and right basal ganglia). For the very similar *Stop Signal* task, the main contrast (stop-go) fails to capture relevant activation besides the sensory activation related to the stop signal itself (presented visually). We find consistent activation for the conflict resolution between stopping a response and ignoring said stop signal, but did not capture consistenly the activation for the putative stop signal effect. For the *Two-by-Two* task, although activation in putative regions of task switching (namely, supplementary motor area and pre-supplementary motor area) can be observed for the task-switch conditions, they are not kept in the contrast. In the original study [38] a 2:1 cue:task mapping is proposed, in order to assess the effect of cue and task switching separately. While the behavioral results were successful, this change turned the task into a more complex and demanding for our participants. Future studies are required to determine if this variation of the task switching paradigm is suited for fMRI mapping of the process.

Following with the *Stroop* task, no robust activation was found on putative areas for the stroop effect (anterior cingulate cortex and dorso-lateral prefrontal cortex).

For the *Attention* task, we found either very weak or absent activation for the orienting and executive control regions described in the original work [9].

The *Discount* task comes from purely behavioral research [21], and is probably more suited for parametric analysis of the conditions than for brain mapping. For the latter, no relevant activations were found in conjunction maps for our participants.

The *Ward and Aliport* task originally seeks to differentiate two different components of planning: what they call "goal hierarchy" and "search depth" [20]. They report in the original work a subtle differentiation in these two concepts in terms of activation: goal hierarchy activates more prominently the left dorso-lateral prefrontal cortex (DLPFC), and search depth activates more prominently the right DLPFC. In our case, we see strong and robust activations for goal hierarchy, with ambiguous trials eliciting far stronger activations than unambiguous ones. Also, the effect of search depth was not adequately captured, as the difference between the 'direct' and 'intermediate' maps is very minor.

The *Columbia Cards* task presents a small locus of activation in the orbitofrontal cortex, but otherwise no activations in areas putatively involved in gambling process.

Lastly, in the *Dot Patterns* task, we observe small activations in dorsal parietal areas, but fail to capture activations mentioned in the original study [25] as responsible for cognitive control in some of the conditions (namely, medial wall of the prefrontal cortex, anterior cingulate, orbitofrontal cortex, and DLPFC).

Some effects in the cognitve regions associated with the processes assumed to take place in the Stanford tasks are not statistically significant. One cannot assert they are not present, only that the small size of the cohort was too small to identify them. Another possible limitation of our analysis is also the lack of adaptations that might be required to adequately use these tasks for brain mapping.

Multi-Voxel Pattern Analysis

In order to assess the quality of the data from the *Realistic Sounds* task, we conducted a multi-voxel pattern analysis (MVPA) to see to what extent activations in the auditory cortex could be differentiated into categories as presented in the stimuli.

The input used for the model referred to the averaged images for all trials of a given condition for a particular run. Since the task was acquired in 12 runs, and there were 6 categories of interest ('silence' and 'catch' categories were

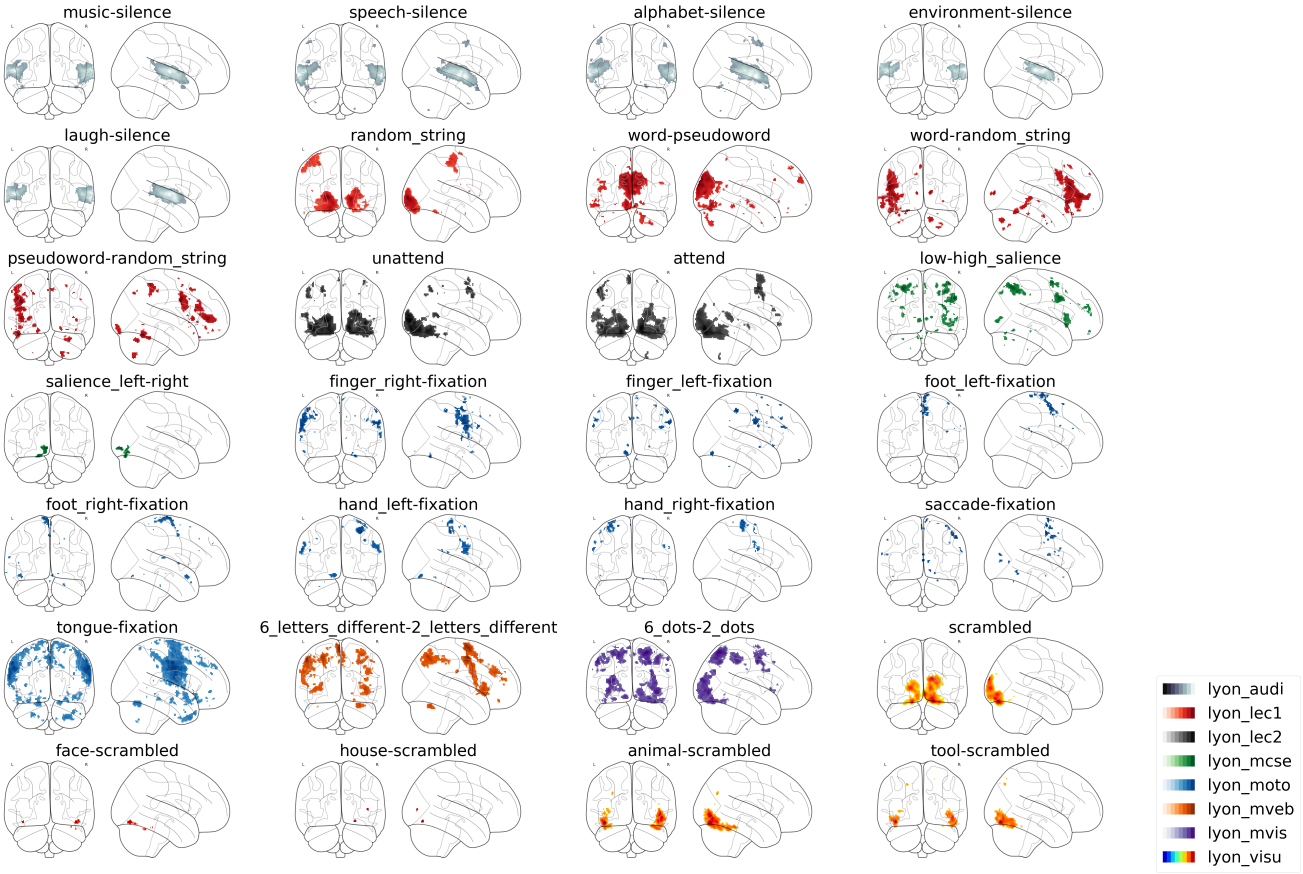

Figure 2. Selection of contrasts for the Lyon battery. Obtained by calculating the conjunction of 25% of the cohort for the main contrasts, robust activation can be observed for all tasks. Correction for multiple comparisons was addressed with an FDR rate set at 5%.

excluded), there were a total of 72 images per participant. Using a Support Vector Classification with linear kernel from scikit-learn [26], the model achieved an mean accuracy of 55% using a stratified K-fold cross-validation strategy (chance=17%). The confusion matrix can be found in Figure 4 for more details on the results. The 'speech' label stands out as the easiest to predict, with a 0.74 prediction accuracy whild being confounded evenly with the rest of the labels, whereas 'animal' and 'tools' are the worst predicted, both reaching a 0.1 confounding rate with several other labels. The rest of the labels ('music', 'nature' and 'voice') have very similar accuracies (0.56, 0.56 and 0.52 respectively). The three of them are most confounded with 'animal', while 'voice' is also similarly confounded with 'speech'.

Data and Software Availability

Source Data

Source data of the present release (plus the former three releases) can be accessed via the public repository *OpenNeuro* [34] under the data accession number *ds*?????? as well as on *EBRAINS* platform (XXXA.L.: Data citations of both collections w/ DOI when available. If the fourth release is published in a new collection together with the previous releases, the list of authors shall account for all authors from all releases.) Previous collections referring to the three first releases can be also found in the OpenNeuro under data accession number *ds*002685 [31] and *EBRAINS* [33]. This collection comprises ∼1.1TB of MRI data.

The NIfTI files as well as paradigm descriptors and imaging parameters are organized per run for each session according to BIDS Specification:

- The data repository is organized in twelve main directories `sub-01` to `sub-15`; we underline that `sub-02`, `sub-03` and `sub-10` are not part of the data and corresponding data from `sub-08` will be made available in further releases
- Data from each subject are numbered on a per-session basis, following the chronological order of the acquisitions; we also note that this order is not the same for all subjects; Table 50 of the IBC documentation can bee consulted for the exact correspondence between Session number and Session ID for every subject on `https://project.inria.fr/IBC/data/` (Session ID's of the present release can be consulted on Table 3 and Session ID's of the first and second releases are respectively provided on Table 2 of [30]);
- Acquisitions are organized within session by modality;

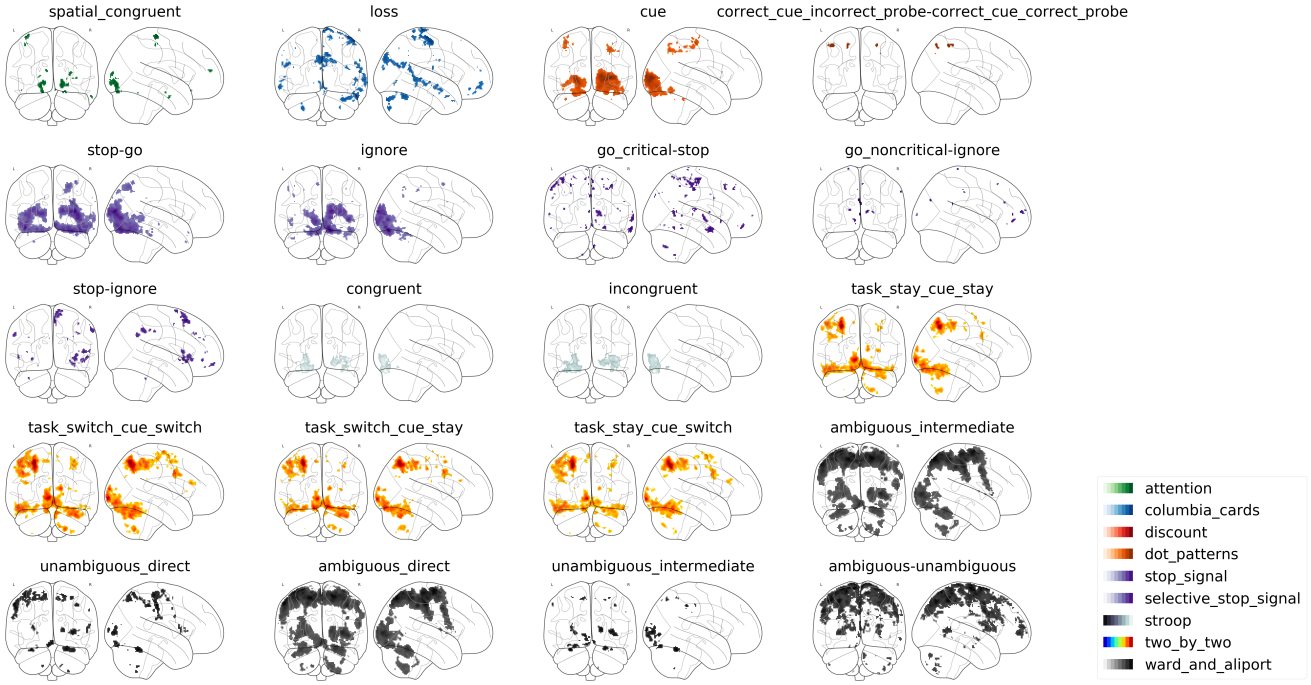

Figure 3. Selection of contrasts for the Stanford battery. Obtained by calculating the conjunction of 25% of the cohort for the main contrasts, robust activation can be observed for all tasks. Correction for multiple comparisons was addressed with an FDR rate set at 5%.

- Different identifiers are assigned to different types of data as follows:
  - gzipped NIfTI 4D image volumes of BOLD fMRI data are named as sub-XX_ses-YY_task-ZZZ _dir-AA_bold.nii.gz, in which XX and YY refer respectively to the subject and session id, ZZZ refers to the name of the task, and AA can be either 'PA' or 'AP' depending on the phase-encoding direction;
  - Event files are named as sub-XX_ses-YY_task-ZZZ_dir-AA_event.tsv;
  - Single-band, reference images are named as sub-XX_ses-YY_task-ZZZ_dir-AA_sbref.nii.gz.

Although BIDS does not yet provide support for data derivatives, a similar directory tree structure was still preserved for this content.

Derived Statistical Maps

The unthresholded-statistic, contrast maps have been released in the public repository *NeuroVault* [13] with the id collection = *XXXX*. A former collection referring to data derivatives from the first, second and third releases is also available in the same repository (id collection = 6618, [32]).

Software

All the protocols used to acquire the IBC dataset are publicly available on the Github repository: https://github.com/hbp-brain-charting/public_protocols.

The code used for data analysis is also publicly available on the following Github repository: https://github.com/hbp-brain-charting/public_analysis_code.

Consent

The experimental procedures were approved by a regional ethical committee for medical protocols in Île-de-France ("Comité de Protection des Personnes" - no. 14-031) and a committee to ensure compliance with data-protection rules ("Commission Nationale de l'Informatique et des Libertés" - DR-2016-033). They were undertaken with the informed written consent of each participant according to the Helsinki declaration and the French public health regulation. Participants were reimbursed on the basis of 80€ per MRI acquisition with extra-fees for any additional session.

Competing interests

No competing interests were disclosed

Grant information

This project has received funding from the European Union's Horizon 2020 Framework Program for Research and Innovation under Grant Agreement No 720270 (Human Brain Project SGA1) and 785907 (Human Brain Project SGA2).

Acknowledgements

We thank the Center for Magnetic Resonance Research, University of Minnesota for having kindly provided the

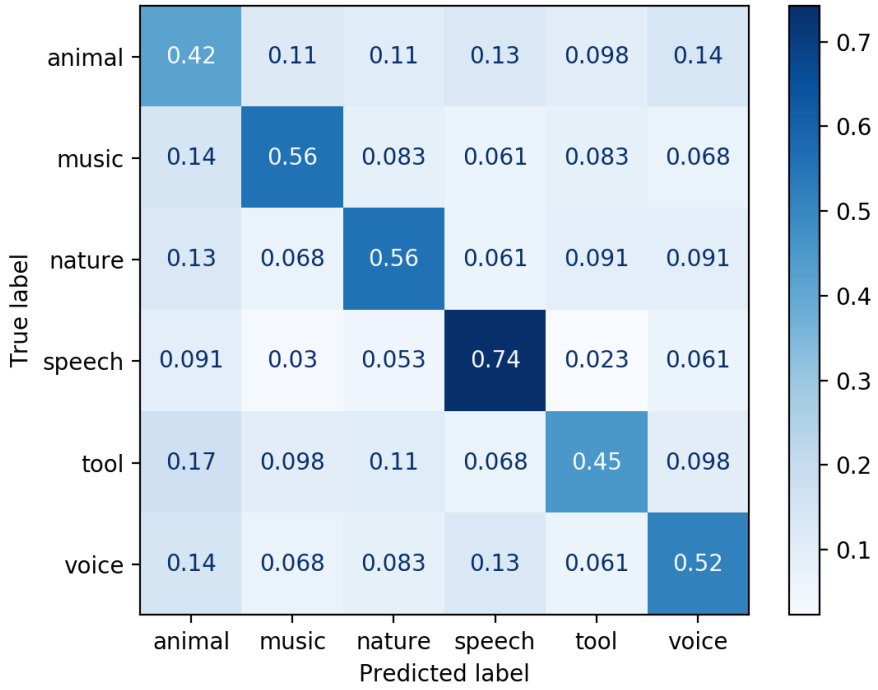

Figure 4. Confusion matrix for multi-voxel pattern analysis of the realistic sounds task. The analysis was performed between-subjects using the contrast maps for each run and each subject

Multi-Band Accelerated EPI Pulse Sequence and Reconstruction Algorithms.

At last, we are especially thankful to all volunteers who have accepted to be part of this challenging study, with many repeated MRI scans over a long period of time.

References

[1] Abraham, A., Pedregosa, F., Eickenberg, M., Gervais, P., Mueller, A., Kossaifi, J., Gramfort, A., Thirion, B., and Varoquaux, G. (2014). Machine learning for neuroimaging with scikit-learn. *Front Neuroinform*, 8:14.

[2] Aron, A. R., Behrens, T. E., Smith, S., Frank, M. J., and Poldrack, R. A. (2007). Triangulating a cognitive control network using diffusion-weighted magnetic resonance imaging (MRI) and functional MRI. *J Neurosci*, 27(14):3743–3752.

[3] Barch, D. M., Burgess, G. C., Harms, M. P., Petersen, S. E., Schlaggar, B. L., Corbetta, M., Glasser, M. F., Curtiss, S., Dixit, S., Feldt, C., Nolan, D., Bryant, E., Hartley, T., Footer, O., Bjork, J. M., Poldrack, R., Smith, S., Johansen-Berg, H., Snyder, A. Z., and Van Essen, D. C. (2013). Function in the human connectome: Task-fMRI and individual differences in behavior. *Neuroimage*, 80:169–89.

[4] Bissett, P. G. and Logan, G. D. (2011). Balancing cognitive demands: control adjustments in the stop-signal paradigm. *J Exp Psychol Learn Mem Cogn*, 37(2):392.

[5] Costafreda, S. (2011). Meta-Analysis, Mega-Analysis, and Task Analysis in fMRI Research. *Philosophy, Psychiatry, & Psychology*, 18:275–277.

[6] Crump, M. J., McDonnell, J. V., and Gureckis, T. M. (2013). Evaluating Amazon's Mechanical Turk as a tool for experimental behavioral research. *PLoS One*, 8(3).

[7] Dockès, J., Poldrack, R. A., Primet, R., Gözükan, H., Yarkoni, T., Suchanek, F., Thirion, B., and Varoquaux, G. (2020). NeuroQuery, comprehensive meta-analysis of human brain mapping. *Elife*, 9:e53385.

[8] Eriksen, B. A. and Eriksen, C. W. (1974). Effects of noise letters upon the identification of a target letter in a nonsearch task. *Percept Psychophys*, 16(1):143–149.

[9] Fan, J., McCandliss, B. D., Sommer, T., Raz, A., and Posner, M. I. (2002). Testing the efficiency and independence of attentional networks. *J Cogn Neurosci*, 14(3):340–347.

[10] Figner, B., Mackinlay, R. J., Wilkening, F., and Weber, E. U. (2009). Affective and deliberative processes in risky choice: age differences in risk taking in the Columbia Card Task. *J Exp Psychol Learn Mem Cogn*, 35(3):709.

[11] Glasser, M. F., Coalson, T. S., Robinson, E. C., Hacker, C. D., Harwell, J., Yacoub, E., Ugurbil, K., Andersson, J., Beckmann, C. F., Jenkinson, M., Smith, S. M., and van Essen, D. C. (2016). A multi-modal parcellation of human cerebral cortex. *Nature*, 536(7615):171–178.

[12] Gorgolewski, K., Auer, T., Calhoun, V., Craddock, C., Das, S., Duff, E., Flandin, G., Ghosh, S., Glatard, T., Halchenko, Y., Handwerker, D., Hanke, M., Keator, D., Li, X., Michael, Z., Maumet, C., Nichols, N., Nichols, T., Pellman, J., Poline, J.-B., Rokem, A., Schaefer, G., Sochat, V., Triplett, W., Turner, J., Varoquaux, G., and Poldrack, R. (2016). The brain imaging data structure: a standard for organizing and describing outputs of neuroimaging experiments. *Sci Data*, 3:160044.

[13] Gorgolewski, K., Varoquaux, G., Rivera, G., Schwarz, Y., Ghosh, S., Maumet, C., Sochat, V., Nichols, T., Poldrack, R.,

Poline, J.-B., Yarkoni, T., and Margulies, D. (2015). NeuroVault.org: a web-based repository for collecting and sharing unthresholded statistical maps of the human brain. *Front Neuroinform*, 9:8.

[14] Gurevitch, J., Koricheva, J., Nakagawa, S., and Stewart, G. (2018). Meta-analysis and the science of research synthesis. *Nature*, 555:175–182.

[15] Hamamé, C. M., Vidal, J. R., Ossandón, T., Jerbi, K., Dalal, S. S., Minotti, L., Bertrand, O., Kahane, P., and Lachaux, J.-P. (2012). Reading the mind's eye: online detection of visuo-spatial working memory and visual imagery in the inferior temporal lobe. *Neuroimage*, 59(1):872–879.

[16] Hanke, M., Adelhöfer, N., Kottke, D., Iacovella, V., Sengupta, A., Kaule, F. R., Nigbur, R., Waite, A. Q., Baumgartner, F., and Stadler, J. (2016). A studyforrest extension, simultaneous fMRI and eye gaze recordings during prolonged natural stimulation. *Sci Data*, 3.

[17] Hanke, M., Baumgartner, F. J., Ibe, P., Kaule, F. R., Pollmann, S., Speck, O., Zinke, W., and Stadler, J. (2014). A high-resolution 7-Tesla fMRI dataset from complex natural stimulation with an audio movie. *Sci Data*, 1.

[18] Hanke, M., Dinga, R., Häusler, C., Guntupalli, J. S., Casey, M., Kaule, F. R., and Stadler, J. (2015). High-resolution 7-Tesla fMRI data on the perception of musical genres–an extension to the studyforrest dataset. *F1000Res*, 4:174.

[19] Humphries, C., Binder, J. R., Medler, D. A., and Liebenthal, E. (2006). Syntactic and Semantic Modulation of Neural Activity During Auditory Sentence Comprehension. *J Cogn Neurosci*, 18(4):665–679.

[20] Kaller, C. P., Rahm, B., Spreer, J., Weiller, C., and Unterrainer, J. M. (2011). Dissociable contributions of left and right dorsolateral prefrontal cortex in planning. *Cereb Cortex*, 21(2):307–317.

[21] Kirby, K. N. and Maraković, N. N. (1996). Delay-discounting probabilistic rewards: Rates decrease as amounts increase. *Psychon Bull Rev*, 3(1):100–104.

[22] Müller, V. I., Cieslik, E. C., Laird, A. R., Fox, P. T., Radua, J., Mataix-Cols, D., Tench, C. R., Yarkoni, T., Nichols, T. E., Turkeltaub, P. E., Wager, T. D., and Eickhoff, S. B. (2018). Ten simple rules for neuroimaging meta-analysis. *Neurosci Biobehav Rev*, 84:151 – 161.

[23] Oldfield, R. C. (1971). The assessment and analysis of handedness: the Edinburgh inventory. *Neuropsychologia*, 9(1):97–113.

[24] Ossandón, T., Vidal, J. R., Ciumas, C., Jerbi, K., Hamamé, C. M., Dalal, S. S., Bertrand, O., Minotti, L., Kahane, P., and Lachaux, J.-P. (2012). Efficient "pop-out" visual search elicits sustained broadband gamma activity in the dorsal attention network. *J Neurosci*, 32(10):3414–3421.

[25] Otto, A. R., Skatova, A., Madlon-Kay, S., and Daw, N. D. (2014). Cognitive control predicts use of model-based reinforcement learning. *J Cogn Neurosci*, 27(2):319–333.

[26] Pedregosa, F., Varoquaux, G., Gramfort, A., Michel, V., Thirion, B., Grisel, O., Blondel, M., Prettenhofer, P., Weiss, R., Dubourg, V., Vanderplas, J., Passos, A., Cournapeau, D., Brucher, M., Perrot, M., and Duchesnay, E. (2011). Scikit-Learn: Machine Learning in Python. *J Mach Learn Res*, 12:2825–2830.

[27] Perrone-Bertolotti, M., Kujala, J., Vidal, J. R., Hamame, C. M., Ossandon, T., Bertrand, O., Minotti, L., Kahane, P., Jerbi, K., and Lachaux, J.-P. (2012). How silent is silent reading? Intracerebral evidence for top-down activation of temporal voice areas during reading. *J Neurosci*, 32(49):17554–17562.

[28] Pinel, P., d'Arc, B. F., Dehaene, S., Bourgeron, T., Thirion, B., Bihan, D. L., and Poupon, C. (2019). The functional database of the ARCHI project: Potential and perspectives. *Neuroimage*, 197:527 – 543.

[29] Pinel, P., Thirion, B., Meriaux, S., Jobert, A., Serres, J., Bihan, D. L., Poline, J.-B., and Dehaene, S. (2007). Fast reproducible identification and large-scale databasing of individual functional cognitive networks. *BMC Neurosci*, 8:91.

[30] Pinho, A. L., Amadon, A., Ruest, T., Fabre, M., Dohmatob, E., Denghien, I., Ginisty, C., Séverine-Becuwe, Roger, S., Laurier, L., Joly-Testault, V., Médiouni-Cloarec, G., Doublé, C., Martins, B., Pinel, P., Eger, E., Varoquaux, G., Pallier, C., Dehaene, S., Hertz-Pannier, L., and Thirion, B. (2018). Individual Brain Charting, a high-resolution fMRI dataset for cognitive mapping. *Sci Data*, 5:180105.

[31] Pinho, A. L., Amadon, A., Ruest, T., Fabre, M., Gauthier, B., Clairis, N., Knops, A., Genon, S., Dohmatob, E., Denghien, I., Torre, J., Ginisty, C., Becuwe-Desmidt, S., Roger, S., Lecomte, Y., Berland, V., Laurier, L., Joly-Testault, V., Médiouni-Cloarec, G., Doublé, C., Martins, B., Salmon, E., Piazza, M., Melcher, D., Pessiglione, M., van Wassenhove, V., Pinel, P., Eger, E., Varoquaux, G., Pallier, C., Dehaene, S., Hertz-Pannier, L., and Thirion, B. (2020a). IBC. OpenNeuro. Dataset. ds002685.

[32] Pinho, A. L., Amadon, A., Ruest, T., Fabre, M., Gauthier, B., Clairis, N., Knops, A., Genon, S., Dohmatob, E., Denghien, I., Torre, J., Ginisty, C., Becuwe-Desmidt, S., Roger, S., Lecomte, Y., Berland, V., Laurier, L., Joly-Testault, V., Médiouni-Cloarec, G., Doublé, C., Martins, B., Salmon, E., Piazza, M., Melcher, D., Pessiglione, M., van Wassenhove, V., Pinel, P., Eger, E., Varoquaux, G., Pallier, C., Dehaene, S., Hertz-Pannier, L., and Thirion, B. (2020b). IBC release 2. NeuroVault. id collection=6618.

[33] Pinho, A. L., Amadon, A., Ruest, T., Fabre, M., Gauthier, B., Clairis, N., Knops, A., Genon, S., Dohmatob, E., Denghien, I., Torre, J., Ginisty, C., Becuwe-Desmidt, S., Roger, S., Lecomte, Y., Berland, V., Laurier, L., Joly-Testault, V., Médiouni-Cloarec, G., Doublé, C., Martins, B., Salmon, E., Piazza, M., Melcher, D., Pessiglione, M., van Wassenhove, V., Pinel, P., Eger, E., Varoquaux, G., Pallier, C., Dehaene, S., Hertz-Pannier, L., and Thirion, B. (2020c). Individual Brain Charting (IBC, release 2). EBRAINS. Dataset.

[34] Poldrack, R., Barch, D., Mitchell, J., Wager, T., Wagner, A., Devlin, J., Cumba, C., Koyejo, O., and Milham, M. (2013). Toward open sharing of task-based fMRI data: the openfMRI project. *Front Neuroinform*, 7:12.

[35] Poldrack, R., Kittur, A., Kalar, D., Miller, E., Seppa, C., Gil, Y., Parker, D., Sabb, F., and Bilder, R. (2011). The Cognitive Atlas: Toward a Knowledge Foundation for Cognitive Neuroscience. *Front Neuroinform*, 5:17.

[36] Saignavongs, M., Ciumas, C., Petton, M., Bouet, R., Boulogne, S., Rheims, S., Carmichael, D. W., Lachaux, J.-P., and Ryvlin, P. (2017). Neural activity elicited by a cognitive task can be detected in single-trials with simultane-

ous intracerebral EEG-fMRI recordings. *Int J Neural Syst*, 27(01):1750001.

[37] Santoro, R., Moerel, M., De Martino, F., Valente, G., Ugurbil, K., Yacoub, E., and Formisano, E. (2017). Reconstructing the spectrotemporal modulations of real-life sounds from fMRI response patterns. *Proc Natl Acad Sci U S A*, 114(18):4799–4804.

[38] Schneider, D. W. and Logan, G. D. (2011). Task-switching performance with 1: 1 and 2: 1 cue–task mappings: Not so different after all. *J Exp Psychol Learn Mem Cogn*, 37(2):405.

[39] Schwartz, Y., Thirion, B., and Varoquaux, G. (2013). Mapping cognitive ontologies to and from the brain. In *NIPS'13: Proceedings of the 26th International Conference on Neural Information Processing Systems*, volume 2 of *NIPS'13*, pages 1673–1681, Red Hook, NY, USA. Curran Associates Inc.

[40] Schwartz, Y., Varoquaux, G., Pallier, C., Pinel, P., Poline, J.-B., and Thirion, B. (2012). Improving Accuracy and Power with Transfer Learning Using a Meta-analytic Database. In Ayache, N., Delingette, H., Golland, P., and Mori, K., editors, *Med Image Comput Comput Assist Interv. 2012*, volume 15, pages 248–255, Berlin, Heidelberg. Springer.

[41] Sengupta, A., Kaule, F. R., Guntupalli, J. S., Hoffmann, M. B., Häusler, C., Stadler, J., and Hanke, M. (2016). A studyforrest extension, retinotopic mapping and localization of higher visual areas. *Sci Data*, 3.

[42] Shallice, T. (1982). Specific impairments of planning. *Philos Trans R Soc Lond B Biol Sci*, 298(1089):199–209.

[43] Stroop, J. R. (1935). Studies of interference in serial verbal reactions. *J Exp Psychol*, 18(6):643.

[44] Varoquaux, G., Schwartz, Y., Poldrack, R., Gauthier, B., Bzdok, D., Poline, J.-B., and Thirion, B. (2018). Atlases of cognition with large-scale brain mapping. *PLoS Comput Biol*, 14(11).

[45] Vidal, J. R., Ossandón, T., Jerbi, K., Dalal, S. S., Minotti, L., Ryvlin, P., Kahane, P., and Lachaux, J.-P. (2010). Category-specific visual responses: an intracranial study comparing gamma, beta, alpha, and ERP response selectivity. *Front Hum Neurosci*, 4:195.

[46] Wager, T. D., Atlas, L. Y., Lindquist, M. A., Roy, M., Woo, C.-W., and Kross, E. (2013). An fMRI-Based Neurologic Signature of Physical Pain. *N Engl J Med*, 368(15):1388–1397.

[47] Wager, T. D., Lindquist, M., and Kaplan, L. (2007). Meta-analysis of functional neuroimaging data: current and future directions. *Soc Cogn Affect Neurosci*, 2(2):150–158.

[48] Ward, G. and Allport, A. (1997). Planning and problem solving using the five disc Tower of London task. *Q J Exp Psychol Section A*, 50(1):49–78.